

Static push-out test on steel and recycled tire rubber-filled concrete composite beams

Qing-Hua Han^{1,2}, Jie Xu^{1,2}, Ying Xing^{*1} and Zi-Lin Li³

¹ School of Civil Engineering, Tianjin University, Tianjin 300072, China

² Key Laboratory of Coast Civil Structure Safety, Tianjin University,
Ministry of Education, Tianjin 300072, China

³ School of Civil Engineering, Tianjin Chengjian University, Tianjin 300384, China

(Received August 27, 2014, Revised February 25, 2015, Accepted March 02, 2015)

Abstract. Recycled tire rubber-filled concrete (RRFC) is employed into the steel-concrete composite structures due to its good ductility and crack resistance. Push-out tests were conducted to investigate the static behavior of steel and rubber-filled concrete composite beam with different rubber mixed concrete and studs. The results of the experimental investigations show that large studs lead a higher ultimate strength but worse ductility in normal concrete. Rubber particles in RRFC were shown to have little effect on shear strength when the compressive strength was equal to that of normal concrete, but can have a better ductility for studs in rubber-filled concrete. This improvement is more obvious for the composite beam with large stud to make good use of the high strength. Besides that the uplift of concrete slabs can be increased and the quantity and width of cracks can be reduced by RRFC efficiently. Based on the test result, a modified empirical equation of ultimate slip was proposed to take not only the compressive strength, but also the ductility of the concrete into consideration.

Keywords: recycled tire rubber-filled concrete; steel-concrete composite beam; push-out test; large studs

1. Introduction

Recycled tire rubber-filled concrete (RRFC) has become a matter of interest for new environmental material in the last few years, duo to its good performance and as an alternative for tire recycling (Siddique and Naik 2004). The rubber particles made from recycled tire in RRFC can not only efficiently improve mechanical property of the concrete, but also ease the potential environment threat. As a combination of concrete and rubber particles, RRFC can provide good behaviors of deformation and crack resistance. Since the first pavement made of RRFC had been built in Arizona State University in 1999, RRFC is widely used in road pavements applications (Zhu *et al.* 2007). Different kinds of tests on samples of RRFC with different volumetric fractions were conducted to investigate the static, dynamic and fatigue mechanical behavior of RRFC. The main conclusions were referred to the optimal crumbed rubber fiber content, the dynamic energy dissipation, the damping capacity and the stiffness reduction of the concrete-rubber composite

*Corresponding author, Ph.D., E-mail: xingying_jamie@163.com

(Hernandez-Olivares *et al.* 2002). Besides the good static and dynamic behaviors of the RRFC, tests conducted by Hernandez-Olivares and Barluenga (2004) also found that crumbed tire rubber additions in structural concrete slabs can improve the fire resistance and driving comfortableness. Güneyisi and Gesoğlu (2014) conducted water absorption, gas permeability, and water permeability tests, and to found that utilization of SF in the rubberized concrete production enhanced the corrosion behavior and decreased corrosion current density values.

As a result of the benefits of combining the advantages of its components, steel–concrete composite beams have been widely used in the high-rise buildings, multi-floor industrial buildings and bridges, which brings good economic and social benefits. The composite action of steel and concrete is realized by the shear connectors welded on the steel flange. The evaluation of the behavior of the shear studs generally takes place with standard push-out test specimens, since the costs and difficulties arise greatly in the full-scale beam tests. A great number of push-out tests were conducted by various researchers to determine the static and dynamic behavior of different shear connectors surrounded in different concrete. Valente and Cruz (2010) studied the performance of steel and lightweight concrete composite beams to obtain a good behavior similar to that of normal density concrete. Zhao and Yuan (2010) conducted several tests to show that the ultimate strength based on Eurocode-4 may be not conservative for predicating the moment capacity of composite beams with high-strength steel and concrete. Tahir *et al.* (2009) performed an investigation on the new stud system fastened with high strength pins and found that the stud system can be improved by increasing the size and the strength of the pins and base plate. Yan *et al.* (2013) carried 102 push out tests to reveal the influence of light-weight concrete, concrete strength and J-hook connectors on the static behavior of composite beam. Ernst *et al.* (2009) studied an approach for the design of secondary composite beam shear connections. Among the recent research, the use of large studs is becoming more and more common with the high strength requires of the modern structures. The composite beam with large studs can also decrease the welding time and makes it easy to remove a deteriorated concrete slab during the maintenance. However, the ductility of large stud may be a key restriction for the application.

In the light of the good static and dynamic behavior of the RRFC and widely used of the steel-concrete composite beam, to employ the RRFC as an alternative for the composite beam can theoretically research a better results. Some previous works also showed that the RRFC and steel composite beam had a better fatigue behavior (Li *et al.* 2015). This research systematically investigates the application of steel-RRFC composite beam. A series of 18 standard push-out tests were developed to study the behavior and applicability of studs with diameter of 16, 19, 22 mm embedded in RRFC. This paper presents the static behavior of push-out specimens made of normal concrete and RRFC with different size of stud respectively. Based on our experiments, failure modes of specimens and cracks of concrete were observed, and ultimate strength, relative slip and shear stiffness of studs in both normal concrete and RRFC were discussed. Moreover, different uplift of concrete slab caused by rubber particles were found and explained by the various stress mechanism of studs embedded in different concrete.

2. Push-out tests program

2.1 Material properties

In order to remove the reduction effect of rubber particles on the compressive strength of the concrete, the compressive strength of RRFC has been raised to the same level as normal concrete

by changing the proportions of other aggregates. A series of mix proportions of RRFC were conducted to determine the best concrete mix proportion before the standard push-out tests. Material characteristic tests of the concrete and steel used in specimens were conducted to obtain the material property and constitutive relation.

A series of tests on RRFC had been conducted to determine the best concrete mix proportion shown in Table 1. The compressive strength of RRFC was improved to almost the same value as normal concrete by changing the usage of other aggregates. For each kind of concrete, six standard prisms with the dimensions of 150 × 150 × 300 mm and six standard cubes with the dimensions of 150 × 150 × 150 mm were prepared at the time the push-out specimens were cast. Half of the cube specimens were cured in the standard curing condition, and the other half of the cube specimens and all prism specimens were cured in the same condition with the push-out specimens. During compress tests of concrete, the failure was so brittle that loading at normal speeds makes the concrete break rapidly soon after compressive strength is reached. As a result, the unloading process was difficult to test. In order to obtain the whole descending part of the stress-strain curve, a frame with very high stiffness was used to share the load with the concrete and keep a very small

Table 1 Concrete mix composition

| Ingredients | Rubber (kg) | Cement (kg) | Sand (kg) | Gravel (kg) | Water (kg) | Water reducing agent (kg) |
|-------------|-------------|-------------|-----------|-------------|------------|---------------------------|
| Concrete | 0 | 400 | 588 | 1277 | 185 | 2.2 |
| RRFC | 50 | 500 | 703 | 1004 | 169 | 4.5 |

Table 2 Mean value of material properties of concrete

| Volumetric fraction of rubber | f_c (28 days with standard curing /MPa) | f_c (at the time of test with air curing /MPa) | $f_{c,u}$ (at the time of test with air curing /MPa) | E (MPa) |
|-------------------------------|--|---|---|--------------------|
| 0% | 49.3 | 52.3 | 36.5 | 3.37×10^4 |
| 5% | 51.8 | 56.3 | 39.2 | 3.22×10^4 |



Fig. 1 Testing equipment of concrete compressive strength test

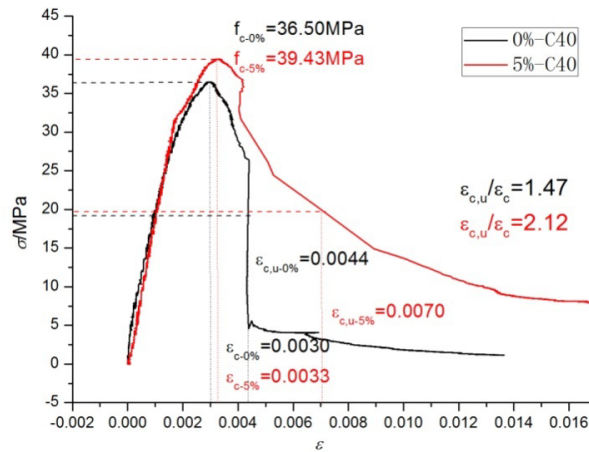


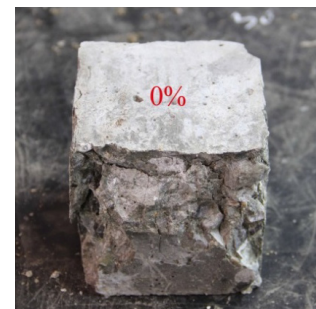
Fig. 2 Stress-strain curves of concrete



(a) Standard prisms



(b) Standard cubes of RRFC



(c) Standard cubes of normal concrete

Fig. 3 Failure mode of concrete

load increment on the concrete prism. The load on the concrete prism was measured by a pressure sensor, and the deformity was tested by an extensometer with a gauge length of 100 mm, as shown in Fig. 1. Table 2 presents the mean compressive strength and modulus of elasticity of concrete tested over 28 days and when the push-out test started, respectively. Fig. 2 shows the stress-strain curves of two kinds of concrete according to the compress tests results using standard prisms.

In Fig. 2, $\varepsilon_c / \varepsilon_{c,u}$ represents the plasticity during failure of the concrete, where ε_c is peak strain, and $\varepsilon_{c,u}$ is the strain when the stress decreases to half of the peak stress. It can be seen that the prism compressive strength and peak strain of both kinds of concrete are almost the same, and the modulus of elasticity of the RRFC with rubber volumetric fraction of 5% is slightly lower than the normal concrete, while the deformation and the plasticity during failure stage is obviously better. The addition of rubber granules made the damage changed from brittle fracture to ductile fracture. The rubber particles can improve the crack resistant of concrete by preventing the propagation of microcracks, whose growth and convergence can lead to through cracks and failure of concrete. The failure modes of concrete presented in Fig. 3 show that RRFC could remain its shape while

the normal concrete was broken completely. Cracks in the RRFC were smaller and uniformly distributed, while the ones in normal concrete were much wider and more fatal.

The structure steel beam of section WH200×200a with the quality of Q235 was used in the tests. From the tensile tests of lath cut from the flange of steel beam, the mean yield strength and ultimate strength were 241 N/mm² and 398 N/mm² respectively. The headed studs used in the tests have material quality of ML15, and the mean ultimate strength was 365 N/mm² according to the tensile tests. Based on the tensile tests on standard bars of 10 mm, the yield strength and ultimate strength can be determined as 348 N/mm² and 455 N/mm² respectively.

2.2 Test specimens

The test specimens were designed refer to Eurocode-4 (2004) with an exception of the number of studs. The specimen consisted of a 550 mm long WH200 × 200a profile steel and two 460 mm long, 400 mm wide and 160 mm thick concrete slabs. The slabs were connected to the steel beam by headed shear studs welded on each side of the steel beam respectively. There were three kinds of studs with diameters of 16 mm, 19 mm, and 22 mm in the tests. The thickness of the concrete slab was more than 7 times the maximum diameter of stud to prevent the slab failure, and all the specimens used the unified size of the slabs for convenient fabrication. The welding collars observed the requirement of EN ISO 13918 (1998). All the specimens had uniform reinforcement and a single row of tow studs embedded in each slab. Bonding at the interface of the concrete slab

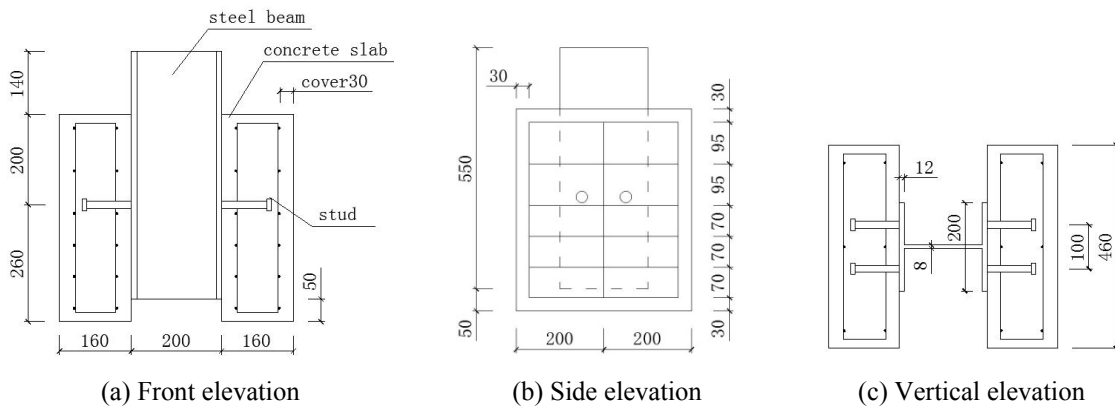


Fig. 4 Details of the push-out test specimens

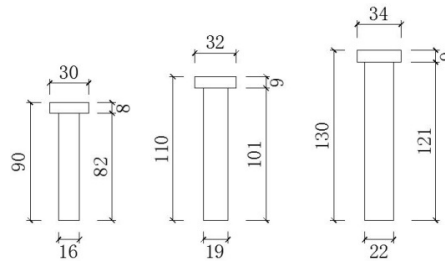


Fig. 5 Details of the studs

Table 3 Summary of the static push-out test specimens

| Series | Specimen | Compressive strength of concrete (MPa) | Volumetric fraction of rubber (%) | Diameter of stud (mm) | Length of stud (mm) | Number of specimens |
|----------|----------|--|-----------------------------------|-----------------------|---------------------|---------------------|
| Series 1 | PS1~3 | 40 | 0 | 16 | 90 | 3 |
| Series 2 | PS4~6 | | 5 | | | 3 |
| Series 3 | PS7~9 | | 0 | 19 | 110 | 3 |
| Series 4 | PS10~12 | | 5 | | | 3 |
| Series 5 | PS13~15 | | 0 | 22 | 130 | 3 |
| Series 6 | PS16~18 | | 5 | | | 3 |

and the steel beam was removed by greasing the beam flange. Each of the concrete slabs was cast in the horizontal position, and the push specimens were cured in a normal environment as is done for composite beams in practice. The test program consisted of two controlled variables including the volumetric fractions of rubber and the stud diameter. Details of the push-out specimens and studs are shown in Figs. 4 and 5 respectively, and the controlled variables are summarized in Table 3.

2.3 Test setup and loading procedures

Monotonic loading was applied by a 1000 kN electro-hydraulic servo testing machine. A steel head plate was set on the top of the beam with its four corners supported to ensure the specimen was compressed concentrically. Load control was used for the monotonic test. The loading setup is shown in Fig. 6.

The monotonic tests were conducted at a load rate of 0.05 kN/s, and the loading was kept constant for 2 minute after reaching the default per stage. The load increment was imposed as 20 kN per stage at the initiation of the test and was changed to displacement control method after



Fig. 6 Loading setup of the push-out test

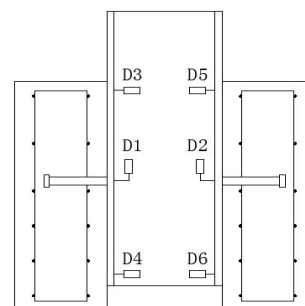


Fig. 7 Measuring point layout of push-out specimen

either the yield characteristic appeared or the loading was up to 90% of the expected ultimate bearing capacity. Failure did not occur in less than 80 minutes, which met the requirements in Eurocode-4. The load produced by the actuator, the displacement of the actuator, the longitudinal slip between each concrete slab and steel beam, and the uplift of the concrete slabs from the steel flange were measured continuously throughout the entire test. The displacement measured by the built-in transducer in the actuator included extra movement due to the compliance of the test rig, so it was larger than the real displacement and was not used in any analysis. The displacement of the actuator was measured by a 1/1000 mm displacement meter under the actuator. The longitudinal slip and uplift were measured respectively by two displacement meters (D1 and D2) with a range of 50 mm and four displacement meters (D3~D6) with a range of 10 mm on the flanges to which the studs were welded. The position of the measuring point and the method of slip measurement are presented in Fig. 7. All the measurements were conducted until the specimen failed.

3. Test results and discussion

Flexible shear connectors like headed studs can prevent brittle failure of concrete slab to ensure good ductility of composite beams. The results from the push-out tests show that the performance of concrete and the diameter of stud have a significant impact on the ultimate bearing capacity and the longitudinal slip of the specimens.

3.1 Ultimate shear strength

The static shear capacity, which is determined by both the performance of the studs and the concrete around them, is the most important property for the design of headed studs. Failure mode of the headed stud shear connector can be stud shank shearing off and shear failure or splitting failure of concrete slab. In order to test the shear capacity of stud, appropriate transverse reinforcement was set to prevent the failure of concrete slab, so the failure modes of all the specimens were shank failure.

The ultimate shear strength and failure mode of each specimen are summarized in Table 4. In the table, P_p and P_u represent the proportional limit load and the ultimate load respectively, and $P_{u,m}$ is the mean value of the ultimate loads from the three test results. For the specimens made of same concrete but different studs, the ultimate load increased with the section area of the stud. The ratio of mean ultimate load to section area $P_{u,m}/A_s$ showed in Fig. 8 represents the utilization level of stud material, and it may remain as a constant value if the ultimate capacity increases with the section area linearly. With P_u/A_s was 99.3%, 87.1%, and 100.2% of the steel material's ultimate strength respectively, Series 1, Series 3, and Series 5 showed basically the same growth rates of bearing capacity. The values of Series 2, Series 4, and Series 6 were 105.9%, 87.8%, and 102.6% respectively. The steel material's strength of studs stated in the manuscript was an average value of a series studs with three diameters. In the material characteristic test, the strength of stud with diameter of 19 mm was proved to be a little less than the ones with the diameters of 16mm and 22 mm, which lead to a smaller P_u/A_s of Series 3 and Series 4. Taken the random error into consideration, it can be determined that the increments of ultimate loads are nearly linear to the section area of the stud, and the studs with diameter of 22 mm, whose section strength is larger than 100% of the steel material's ultimate strength, have enough bearing capacity .

In addition, there was an obvious declining trend of P_p/P_u with the increment of stud diameter,

and the mean value of P_p/P_u is 62.1% for stud of $\phi 16$, 58.8% for $\phi 19$, and 50.4% for $\phi 22$. It means the elastic stage shared a lesser proportion in the overall loading process, which leads to early decreasing of shear stiffness.

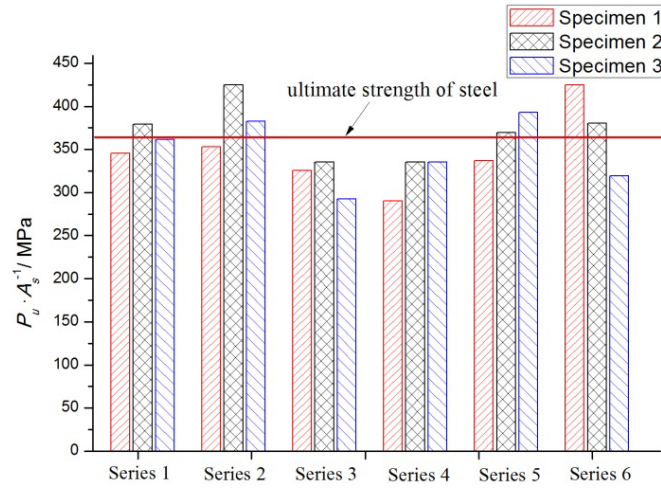


Fig. 8 P_u/A_s of shear connectors

Table 4 Static push-out test results

| Series | Specimen | Ultimate strength per stud (kN) | | P_p/P_u (%) | $P_{u,m}$ (kN) | $P_{u,m}/A_s$ (MPa) | Failure mode |
|----------|----------|---------------------------------|-------|------------------|-------------------|------------------------|---------------------|
| | | P_p | P_u | | | | |
| Series 1 | PS-1 | 45.5 | 69.5 | 65.0 | | | shank failure |
| | PS-2 | 47.4 | 76.2 | 62.2 | 72.8 | 362.3 | shank failure |
| | PS-3 | 43.8 | 72.6 | 60.3 | | | shank failure |
| Series 2 | PS-4 | 45.2 | 70.9 | 63.8 | | | shank failure |
| | PS-5 | 50.2 | 85.3 | 58.9 | 77.7 | 386.6 | shank failure |
| | PS-6 | 48.1 | 76.9 | 62.5 | | | shank failure |
| Series 3 | PS-7 | 57.1 | 92.3 | 61.9 | | | shank failure/crack |
| | PS-8 | 54.9 | 95.0 | 57.8 | 90.1 | 317.9 | shank failure |
| | PS-9 | 59.9 | 82.9 | 72.3 | | | shank failure |
| Series 4 | PS-10 | 40.9 | 82.3 | 49.7 | | | shank failure |
| | PS-11 | 56.5 | 95.1 | 59.4 | 90.8 | 320.4 | shank failure |
| | PS-12 | 49.3 | 95.0 | 51.9 | | | shank failure |
| Series 5 | PS-13 | 72.2 | 128.1 | 56.4 | | | shank failure/crack |
| | PS-14 | 60.6 | 140.5 | 43.1 | 139.0 | 365.8 | shank failure/crack |
| | PS-15 | 70.2 | 149.2 | 47.1 | | | shank failure |
| Series 6 | PS-16 | 70.2 | 144.4 | 48.6 | | | shank failure/crack |
| | PS-17 | 75.9 | 161.4 | 47.0 | 142.3 | 374.5 | shank failure |
| | PS-18 | 73.3 | 121.3 | 60.4 | | | shank failure |

Increment of ultimate load caused by RRFC can be found by comparing the results of Series 1 against Series 2, Series 3 against Series 4, and Series 5 against Series 6. The increment of mean ultimate load was minimal with the largest gap was only 6.7% as shown in Series 1 and Series 2. In fact, the compressive strength of both kinds of concrete was not exactly the same. The compressive strength of RRFC and normal concrete was 39.2 MPa and 36.5 MPa respectively, and the gap was 7.4%, which is almost the same as the gap of the ultimate strength of push-out specimens. Therefore, the slight difference in the ultimate capacity of specimens may be attributed to their different compressive strengths of materials. This reflects that if the compressive strength of normal concrete and RRFC is equal, the bearing capacity of the push-out specimens is not affected by the addition of rubber particles.

3.2 Ductility and shear stiffness

Ductility is a basic concept in the design, which is represented through ultimate slip. For large studs, ultimate slip is very important for their practical usage in steel–concrete composite bridges. Various diameters of studs lead to different ultimate slip. The ratio of ultimate slip to diameter $\delta_{u,m}/d$, which represents relative deformability of studs with different diameters, was analyzed to compare the deform capacity of different studs. In general, a composite beam can be considered ductile if the connectors can be shown to have a characteristic slip capacity exceeding 6 mm. By experience, the ultimate slip is 1/3 of the diameter. Table 5 summarizes the proportional slip,

Table 5 Relative slip and stiffness of stud connectors

| Series | Specimen | Relative slip (mm) | | | $\delta_{u,m}$ (mm) | $\delta_{u,m}/d$ | $\delta_{u,m}/\delta_{m,m}$ | K (kN/mm) |
|----------|----------|--------------------|------------|------------|------------------------|------------------|-----------------------------|----------------|
| | | δ_p | δ_m | δ_u | | | | |
| Series 1 | PS-1 | 2.2 | 6.7 | 7.7 | | | 20.7 | |
| | PS-2 | 1.0 | 4.1 | -- | 6.3 | 1/2.5 | 47.4 | |
| | PS-3 | 1.2 | 3.3 | 4.9 | | | 36.5 | |
| Series 2 | PS-4 | 0.9 | 4.7 | 7.0 | | | 50.2 | |
| | PS-5 | 0.3 | 5.0 | 6.3 | 6.7 | 1/2.4 | 167.3 | |
| | PS-6 | 1.3 | 4.4 | -- | | | 37.0 | |
| Series 3 | PS-7 | 0.7 | 4.4 | 4.8 | | | 63.4 | |
| | PS-8 | 0.6 | 7.2 | 7.8 | 6.6 | 1/3.7 | 91.5 | |
| | PS-9 | 0.5 | 6.7 | 7.3 | | | 133.1 | |
| Series 4 | PS-10 | -- | -- | -- | | | -- | |
| | PS-11 | 1.5 | 8.6 | 12.6 | 13.2 | 1/1.4 | 37.7 | |
| | PS-12 | 2.6 | 9.9 | 11.9 | | | 19.0 | |
| Series 5 | PS-13 | 1.0 | 5.4 | 6.1 | | | 72.2 | |
| | PS-14 | 0.7 | 8.1 | 9.5 | 7.5 | 1/2.9 | 86.6 | |
| | PS-15 | 0.8 | 5.3 | 6.8 | | | 87.8 | |
| Series 6 | PS-16 | 0.9 | 10.5 | 12.9 | | | 78.0 | |
| | PS-17 | 1.0 | 8.3 | 10.9 | 11.9 | 1/1.8 | 75.9 | |
| | PS-18 | 1.0 | 5.6 | -- | | | 73.3 | |

ultimate slip, ratio of ultimate slip to diameter, and shear stiffness of 18 specimens. In Table.5, δ_p and δ_m represent the longitudinal relative slip corresponding to the proportional limit load and ultimate load respectively, and δ_u represents the slip when the load had reduced to 90% of its peak respectively. K is the initial shear stiffness defined as the ratio of P_p and δ_p .

In order to compare the results of the push-out tests, average load versus longitudinal slip curves of three same specimens in each of the series are shown in Fig. 9. It can be seen that the longitudinal slip increased linearly with the load before it was up to the proportional limit load,

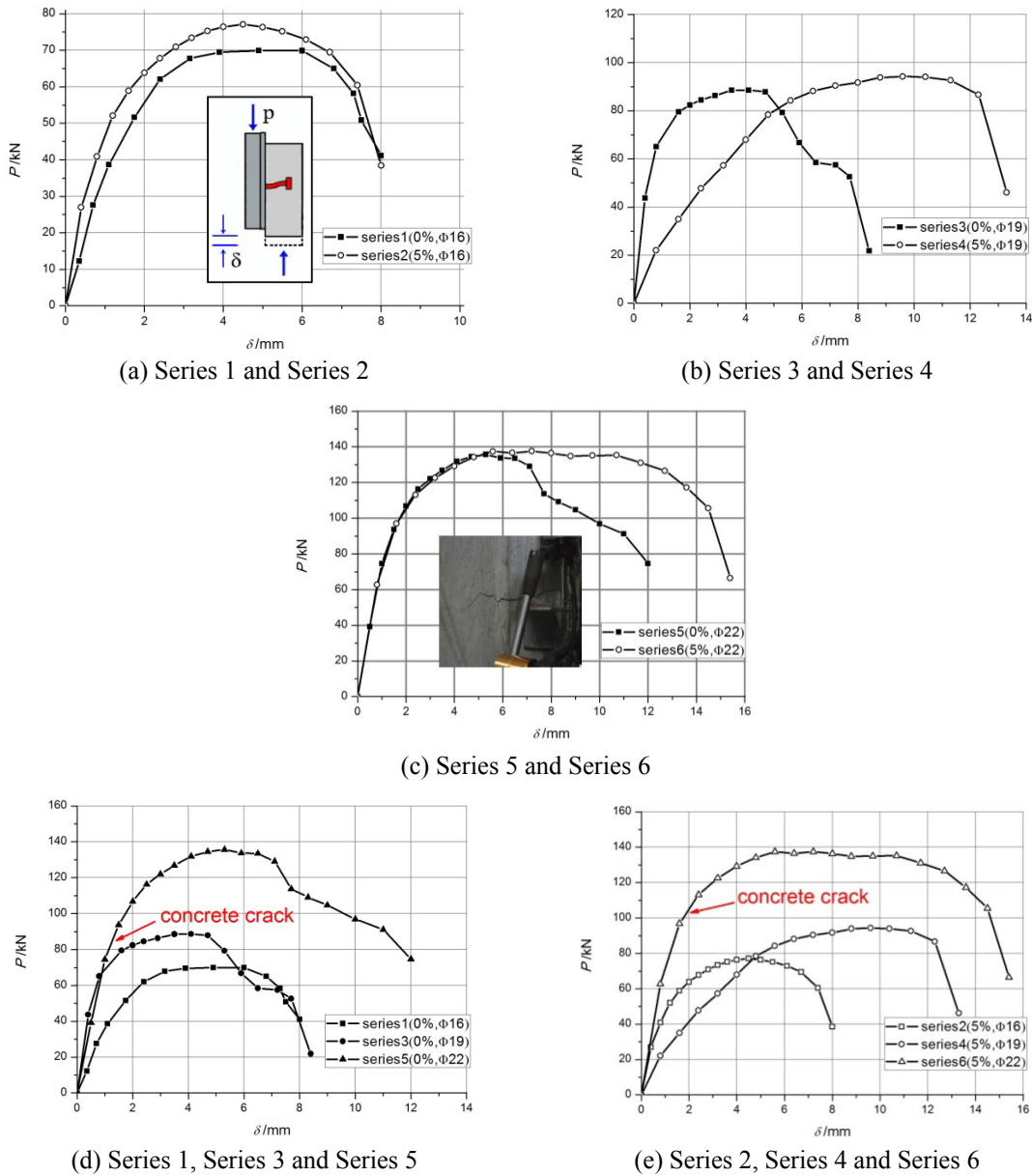


Fig. 9 Load-slip curves

and then the slip increased more quickly while the stiffness of slip decreased significantly. After the ultimate load, the composite effect was almost lost and the slip increased rapidly until complete failure.

Three specimens in the tests had brittle failure and abrupt load decreasing soon after the peak load was reached due to the over quick loading, so their ultimate slips had less reference value. Results in Table 5 and Fig. 9 show that most specimens in the tests had ultimate slip larger than 6mm except for three specimens. Comparing the $\delta_{u,m}$ of Series 1 with Series 2, Series 3 with Series 4, and Series 5 with Series 6 respectively, it can be seen that the ultimate slip of the specimens used in RRFC were larger than those in normal concrete.

Ductility, which is defined by $\delta_{u,m}/d$, were 1/2.6, 1/3.7 and 1/2.8 for the specimens with normal concrete and different studs in Series 1, Series 3 and Series 5. It means that there is a small reduction of ductility for larger studs of $\phi 22$ and $\phi 19$ compared to studs of $\phi 16$ if they are used in normal concrete. In contrast, for the specimens with RRFC, $\delta_{u,m}/d$ were 1/2.4, 1/1.4, and 1/1.8 in Series 2, Series 4, and Series 6 respectively, showing a growing tendency of ductility. It can be concluded that a stud of $\phi 22$ had a lower ductility than a smaller stud in normal concrete, but RRFC can improve the ductility of large stud effectively. Moreover, the improvement of ductility caused by RRFC depends on the diameter of the stud. For the studs with diameters of 16 mm, 19 mm, and 22 mm, the ductility improvement was 8.3%, 164.3%, and 55.6% respectively. The enhancement of ductility due to rubber particles is more obvious for studs with diameters larger than 16 mm.

$\delta_{u,m}/\delta_{m,m}$ represents the deformability when failure occurs. It is expected that a larger value of $\delta_{u,m}/\delta_{m,m}$ will indicate, a lesser displacement created during a normal situation, but a larger deformation during failure. The results show that the $\delta_{u,m}/\delta_{m,m}$ for studs of $\phi 16$ and $\phi 19$ embedded in normal concrete was 1.30, while it was only 1.18 for studs of $\phi 22$, which means a poor deformability. On the contrary, the $\delta_{u,m}/\delta_{m,m}$ of $\phi 22$ in RRFC was 1.46, which is larger than the value of 1.43 for $\phi 16$ and $\phi 19$. It is also proved that the worse deformability of the larger stud can be improved by RRFC which provide a possibility for the application of even larger studs. All the results of push-out tests are consistent with the material properties obtained from the compress tests of concrete.

The initial shear stiffness are easily to be discrete because the linear elastic stage of $P-\delta$ curve is relatively short, and the measured slip are typically very small values which may get affected by many factors such as the stud weld quality, compaction rate of concrete, eccentric loading, etc. Moreover, one of the specimens in Series 4 had weld defect at the root of studs, which lead to a quite smaller stiffness for Series 4. Although there is discreteness in the shear stiffness, some regulations can still be found. It can be observed from the results in Table 5 and Fig. 9, shear stiffness of stud connectors embedded in RRFC was lesser than that of the studs in normal concrete because of the larger deformation capacity of RRFC. However, the difference of the stiffness can have slight impact on the behavior of composite beams (Shim *et al.* 2004).

3.3 Uplifts of concrete slab

According to the conclusion of the push-out tests conducted before, the slabs connected to the steel beams may deform in two probable modes as shown in Fig. 10. Both modes indicate a tendency of the uplift of the concrete slabs. The load transferred by studs from steel beams to concrete slabs leaves the slabs in small eccentric compressive state, which lead to the deformation in the first mode. On the contrary, transverse deformation of the steel beam in compression can

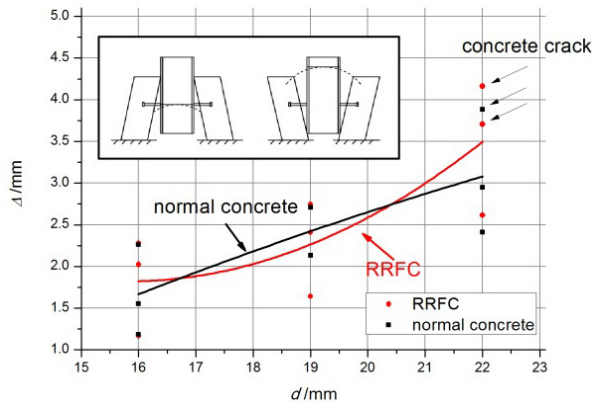


Fig. 10 Uplift of concrete slab versus diameter of stud

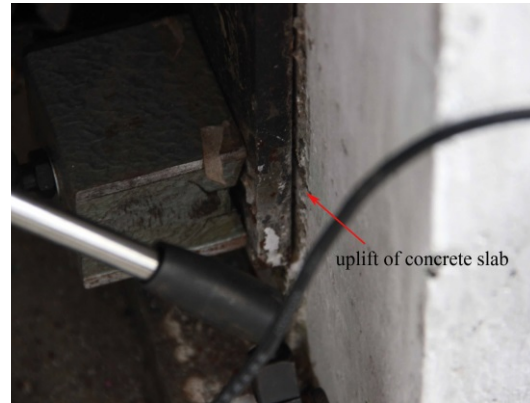


Fig. 11 Uplift of concrete slab

produce a reverse bending, which may lead to the deformation in the second mode. In fact, the deformation modes were affected by fabrication errors, density degrees of concrete below studs, and eccentric loads. Test data obtained from four displacement meters set on flanges to which the studs were welded indicated that most of the specimens deformed into the first mode with a larger uplift at the bottom of the concrete slabs, and only two of them deformed in opposite tendency. According to the test scenario described in Fig. 11, uplift distribution varied linearly along the interface and reached maximum at the bottom of the steel beam. As the load increased, the low part of the concrete slab was separated from the steel beam completely, so the studs embedded in the slab were subjected to the combined action of the tension and the shear force throughout the test.

The tests results show a large dispersion in the uplift values of concrete slabs. It may be caused by the unequal load on each stud in one specimen and different covering layers made of epoxy resin to protect strain gages on the stud, which weakened the resistant effect of stud head against uplifting. However, there is still a nontypical binomial growth in uplifting with respect to the diameter of stud in RRFC, and the increment of uplifting is nearly linear with the increase in diameter of stud in normal concrete as shown in Fig. 10. Larger slip of stud led to larger deformation and uplift of concrete slab, so slabs made of RRFC had a more obvious uplift which corresponds to their larger longitudinal slip. The different uplift of two kinds of concrete can be explained by the forced mechanism of studs in them. The deformations of studs embedded in the normal concrete and RRFC can be seen in Fig. 12. Because of the unique performance of the concrete, the stud in RRFC had a bending deformation in the area two-fifths to the root of the stud, while the stud in normal concrete had it in the area a quarter to the root. The reacting forces provided by concrete at the root and head of the stud were in opposite directions, and the bending moment caused by the reacting forces led to the uplifting of the concrete slabs. For one stud, the reacting force on a certain cross section of the stud is proportional to the bending deformation there, which is shown in Fig. 13(a). For studs with the same diameter, both the value and distribution area of the reacting force provided by RRFC are larger than normal concrete, and the distribution area can be simplified, as is shown in Fig. 13(b). Although the larger deformation area of the stud embedded in RRFC makes its resultant force closer to the axis of the slab, an even larger resultant force still leads to a larger bending moment. As a result, more uplift appeared in the slab made of RRFC.



Fig. 12 Deformation of the stud in RRFC and normal concrete

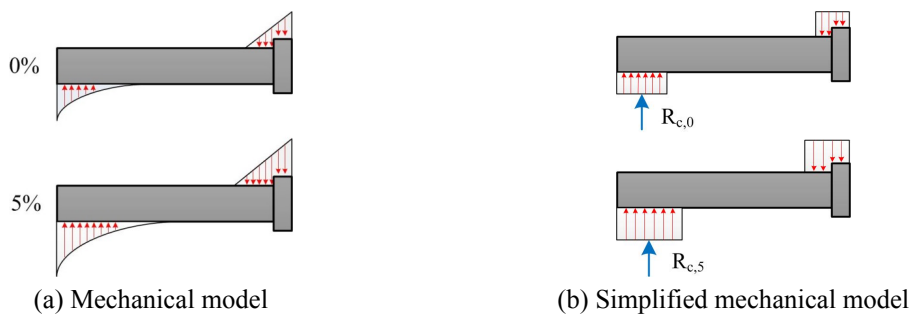


Fig. 13 Mechanical model of stud

As shown in Fig. 10, for all three specimens with extremely large uplift in Series 5 and Series 6, concrete slabs cracked distinctly during the tests, while no cracks appeared on other specimens in Series 5 and Series 6 with smaller uplift. It can be concluded that the uplift of the concrete slab have a close relationship with concrete cracks. Concrete cracks more easily due to the tension caused by the uplift, and overlarge uplift may even lead to embedment failure.

3.4 Failure modes

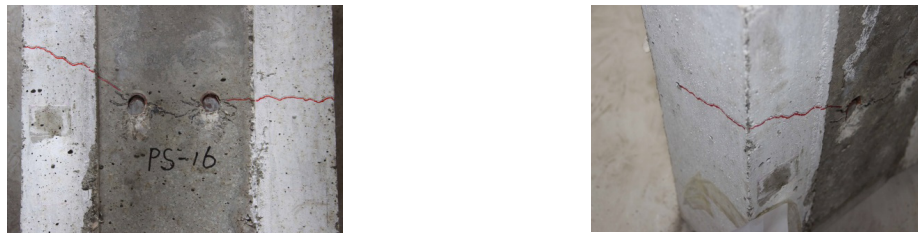
All the failure of static push-out specimens was caused by shear failure of stud shank. For most of the specimens, only two studs in one side were sheared off with the slab separated from the steel beam completely, and the other slab was still connected to the steel beam. There was not any crack on concrete slabs of specimens in Series 1, Series 2 and Series 4, while cracks appeared in both slabs of three specimens in Series 5 and Series 6, and just in a single slab of one specimen in Series 3. The comparison of the failure modes of specimens with different studs and the same concrete shows that concrete strength was enough for studs of $\phi 16$ to avoid any cracks, while studs of $\phi 19$ matched concrete of C40 well and would rarely cause concrete cracks. The concrete had obvious cracks in some specimens using studs of $\phi 22$, but the final failure mode was still shank failure. So concrete crack will not lead to brittle failure, and have little effect on the ultimate bearing capacity of stud.

Fig. 14 presents the concrete cracks of specimens of Series 5 and Series 6. Crack initiation all occurred at the edge of holes in which studs were embedded at the middle of concrete slabs, and

then extended to the margin of slab. There were also cracks between the two studs and at lateral side of the concrete slabs. It can be seen from Fig. 14 that the number of concrete cracks of PS-13 is more than that of PS-16, and the cracks between the two studs of PS-16 are smaller and denser than the cracks of PS-13. During the test, the sound of tearing of the concrete was heard, and tiny cracks were visible when 62% of the P_u was reached for the specimens of Series 5, while 69% of



(a) Concrete cracks of Series 5



(b) Concrete cracks of Series 6

Fig. 14 Failure modes of Series 5 and Series 6

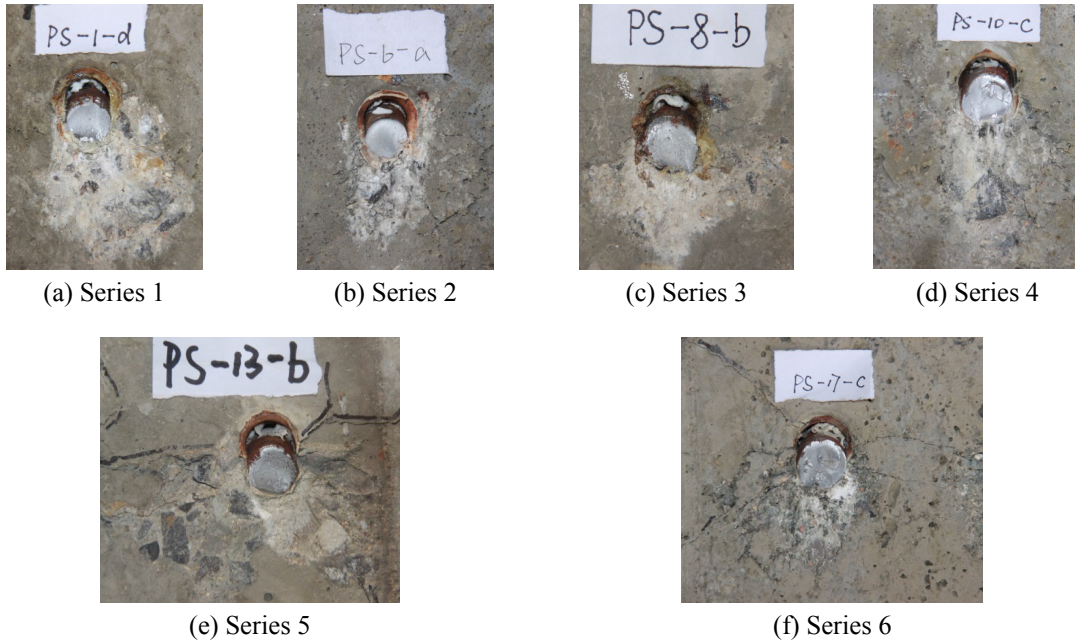


Fig. 15 Local crushing of concrete

the P_u for the specimens of Series 6. Even though the probability of slab crack increases with larger deformation of stud, it is proven that RRFC used in the specimens can delay the appearance of cracks and reduce the amount and width of concrete cracks

Test data indicates that the four studs in a specimen cannot shear off at the same time since the gaps between the studs and the slabs are not the same, which leads to different amounts of plastic deformation. The concrete was damaged partially below the shank, and the damage was most severe around the studs which failed first. Fig. 15 describes the local crushing of concrete below the studs. For the specimens with same studs, the areas of local crushing with normal concrete were almost double of those with RRFC. It is proven that the specimens with RRFC have a better local cracking resistance.

4. Evaluation of the equations

4.1 Comparison with current design codes

Static bearing capacity is essential for the design of headed stud shear connector in composite beam. The ultimate strength per stud for Series 1- Series 6 obtained from the static push-out tests was compared with the shear resistance calculated using the empirical model in the design codes of Eurocode-4 and AASHTO LRFD (2004). In Eurocode-4, the shear resistance of one stud shear connector is determined by the minimum of Eqs. (1) and (2), which present the shear resistance of “failure of the stud” and “failure of the concrete” respectively.

$$P_{Rd} = 0.8f_u(\pi d^2 / 4) / \gamma_v \quad (1)$$

$$P_{Rd} = 0.29\alpha d^2 \sqrt{(f_{ck} E_{cm})} / \gamma_v \quad (2)$$

where f_u is the ultimate strength of steel, d is the diameter of stud, α is the length influence factor of stud determined as $\alpha = 0.2(h/d + 1) \leq 1$, h is the length of stud, f_{ck} is the compressive strength of concrete, E_{cm} is the elastic modulus of concrete, and γ_v is a partial safety factor valued as 1.25. It is assumed that the shear resistance is determined solely by shear resistance of stud shank or compressive capacity of concrete, and interaction between the two materials is ignored.

In AASHTO LRFD, the shear resistance of one stud shear connector is determined by Eq. (3) with the same assumption in Eurocode-4.

$$Q_r = \phi 0.5 A_{sc} \sqrt{(f_{ck} E_{cm})} \leq \phi A_{sc} f_u \quad (3)$$

where ϕ is a resistance factor for shear connector with a value of 0.85, A_{sc} is the cross section area of stud shear connector.

Fig. 16 shows the comparison of shear capacity obtained from tests and that calculated by design codes. It can be observed that all the shear capacities of studs obtained from tests are larger than those calculated based on the Eurocode-4 and Chinese code, while consistent better with AASHTO LRFD. So Eurocode-4 and Chinese code for design of steel structures is conservative in prediction of shear capacity, while AASHTO LRFD is the most suitable one. What's more, even though the design codes do not apply to RRFC and large studs with a diameter larger than 19 mm,

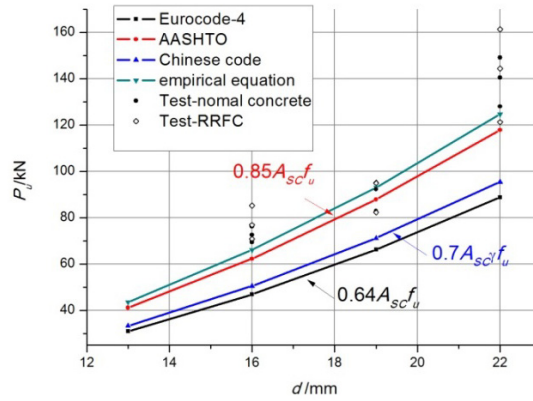


Fig. 16 Comparison of test and design codes

the three codes can still be used for the estimation of the shear capacity of large studs with a diameter of 22 mm and composite beam made of RRFC according to the tests.

4.2 Modification of equation of ultimate slip

Shim *et al.* (2000) analyzed 18 push-out tests, which used different sizes of studs, and suggested the empirical equation of ultimate slip as Eq. (4).

$$\delta_u = (0.48 - 0.0042 f_c) d \tag{4}$$

It can be concluded from the test that, not only compressive strength of concrete but also its deformability during failure has an obvious impact on ultimate slip of stud. Although the empirical equation above can calculate the ultimate slip of stud in normal concrete properly, the deformability of concrete after failure had not been taken into consideration. In order to describe the increment of ultimate slip caused by RRFC, a plastic amplification coefficient μ was introduced and the equation was modified as Eqs. (5) and (6).

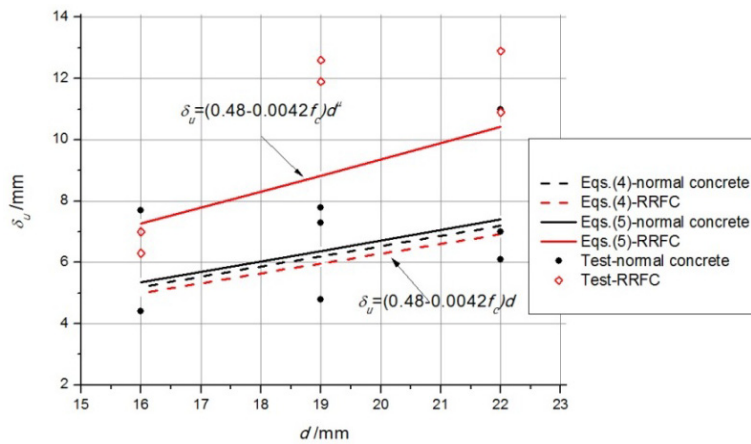


Fig. 17 Comparison of test and modified empirical equations

$$\delta_u = (0.48 - 0.0042 f_c) d^\mu \quad (5)$$

$$\mu = 0.19 \frac{\varepsilon_{c,u}}{\varepsilon_c} + 0.73 \geq 1 \quad (6)$$

where ε_c is the peak strain, and $\varepsilon_{c,u}$ is the strain when stress decreased to half of the peak stress. The ultimate slip measured from tests was compared with the modified empirical equations, as shown in Fig. 17, and the modified equation is consistent with the measured values pretty well.

5. Conclusions

Standard push-out tests for the steel-concrete composite beams with normal and rubber-filled concretes were performed. The ultimate strength, ultimate slip and shear stiffness of stud were investigated and following conclusions have been drawn:

- The compressive strength of RRFC can be the same as that of normal concrete, but RRFC can have better ductility and crack resistance due to its larger deformability during failure.
- The ultimate shear capacity is mainly determined by the stud, and cannot be affected by rubber particles. On the contrary, the shear stiffness of the stud embedded in RRFC is lower than that in normal concrete, and the larger relative slip must lead to a larger uplift of the concrete slab.
- Studs with diameter of 22 mm in normal concrete have enough ultimate strength but less relative slip, smaller elastic stage and worse ductility than these of the smaller studs with diameter of 16 mm and 19 mm. Therefore, it is difficult to make good use of the high strength of the large studs in normal concrete in practical applications. However, with the help of RRFC, ductility of studs has been improved effectively and the improvement is more obvious for large studs so that it is possible to apply large studs into practice.
- Test results show that failure mode of push-out specimens were all shank failure. Even though large studs with diameter of 22 mm can lead to concrete crack, it has little effect on ultimate shear capacity of stud. Moreover, RRFC can reduce the quantity and width of cracks efficiently.
- It has been proved that current codes are still valid for the RRFC and large stud, and the recommended design strength of shear connection in Eurocode-4 is relatively conservative. The ultimate slip capacity of studs in normal concrete is consistent with that of the empirical equation, which has been modified to calculate the better ductility of studs in RRFC.

Acknowledgments

The authors gratefully acknowledge the financial support from the Nature Science Foundation of China (No. 51178307 and No. 51408408).

References

AASHTO LRFD (2004), Bridge design specifications, (3rd Ed.), American Association of State Highway and Transportation Officials.

- EN ISO 13918 (1998), Welding — studs and ceramic ferrules for arc stud welding.
- EN 1994-2 (2004), Eurocode 4: Design of composite steel and concrete structures. Part 2: General rules and rules for bridges; Brussels, Belgium.
- Ernst, S., Bridge, R.Q. and Wheeler, A. (2009), “Push-out tests and a new approach for the design of secondary composite beam shear connections”, *J. Construct. Steel Res.*, **65**(1), 44-53.
- Güneyisi, E. and Gesoğlu, M. (2014), “Experimental investigation on durability performance of rubberized concrete”, *Adv. Concrete Construct., Int. J.*, **2**(3), 187-201.
- Hernandez-Olivares, F. and Barluenga, G. (2004), “Fire performance of recycled rubber-filled high-strength concrete”, *Cement Concrete Res.*, **34**(1), 109-117.
- Hernandez-Olivares, F., Barluenga, G., Bollati, M. and Witoszek, B. (2002), “Static and dynamic behaviour of recycled tyre rubber-filled concrete”, *Cement Concrete Res.*, **32**(10), 1587-1596.
- Li, Z.L., Xing, Y., Han, Q.H. and Guo, Q. (2015), “Fatigue behavior analysis and life prediction of elastic concrete and steel composite beam”, *J. Southeast Univ. (Nature Science Ed.)*, **45**(1), 165-171.
- Shim, C., Kim, J. and Chang, S.P. and Chung, C.H. (2000), “The behaviour of shear connections in a composite beam with a full-depth precast slab”, *Proceedings of the ICE-Structures and Buildings*, **140**(1), 101-110.
- Shim, C., Lee, P. and Yoon, T.Y. (2004), “Static behavior of large stud shear connectors”, *Eng. Struct.*, **26**(12), 1853-1860.
- Siddique, R. and Naik, T.R. (2004), “Properties of concrete containing scrap-tire rubber—an overview”, *Waste Manag.*, **24**(6), 563-569.
- Tahir, M.M., Shek, P.N. and Tan, C.S. (2009), “Push-off tests on pin-connected shear studs with composite steel-concrete beams”, *Construct. Build. Mater.*, **23**(9), 3024-3033.
- Valente, M.I. and Cruz, P.J. (2010), “Experimental analysis on steel and lightweight concrete composite beams”, *Steel Compos. Struct., Int. J.*, **10**(2), 169-185.
- Yan J.B., Liew, J.Y.R., Soheli K.M.A. and Zhang, M.H. (2013), “Push-out tests on J-hook connectors in steel-concrete-steel sandwich structure”, *Mater. Struct.*, **47**(10), 1693-1714.
- Zhao, H.L. and Yuan, Y. (2010), “Experimental studies on composite beams with high-strength steel and concrete”, *Steel Compos. Struct., Int. J.*, **10**(5), 373-383.
- Zhu, H., Liu, C.S., Zhang, Y.M. and Li, Z.G. (2007), “Effect of crumb rubber proportion on compressive and flexural behavior of concrete”, *J. Tianjin Univ.*, **40**(7), 761-765.